

Invited Paper

# Pulsed thermal NDT in tables, figures and formulas

V.P. Vavilov<sup>\*\*\*1</sup>, D.D. Burleigh<sup>\*\*\*</sup>

\* Tomsk Polytechnic University, 634028, Tomsk, Savinykh St., 7, Russia

\*\* Tomsk State University, 634050, Tomsk, Lenin Av., 36, Russia

\*\*\* La Jolla Cove Consulting, San Diego CA 92117, USA

## ABSTRACT

Several reviews and summary papers describing the history and the current status of pulsed thermal nondestructive testing (TNDT) have been published recently. However, some of the theoretical possibilities cannot easily be implemented in practical applications. This paper contains useful tables and formulas that are illustrated with typical IR thermograms to provide a general overlook of pulsed TNDT.

**Keywords:** thermal nondestructive testing, modeling, data processing, heat conduction

## 1. INTRODUCTION

Reviews on thermal nondestructive testing (TNDT) can be found in References [1-14]. A general review of the history of infrared (IR) technology is shown in Table 1. Terminology used in TNDT is shown in Table 2.

Table 1. IR technology and TNDT in short: historical milestones (adapted from [14])\*

<b>BCE.</b> The existence of thermal rays was hypothesized by Titus Lukretius Carus (99 – 55 BCE), a Roman poet and the author of the epic «De Rerum Natura» («On the Nature of the Universe»).
<b>1770.</b> Pictet, a French scientist, described his famous experiment on focusing heat and cold.
<b>1800.</b> Official credit to the discovery of IR radiation is paid to Sir William Herschel.
<b>1840.</b> John Herschel, the William's son, proposed the prototype of an evaporograph and introduced the term «thermogram».
<b>1900s.</b> Einstein, Kirchhoff, Planck, Wien et al. discovered the laws of thermal radiation.
<b>1934.</b> Holst constructed the image converter tube (wavelength range up to 1.5 μm).
<b>1935.</b> Nichols: IR radiometric analysis of hot rolled metals.
<b>1937.</b> Vernotte: Determination of material thermal properties in a dynamic thermal process.
<b>1940s.</b> Night vision equipment. IR photodetectors.
<b>1948.</b> Parker and Marshall: Analysis of temperature distribution in brake shoes.
<b>1949.</b> Gorrill: Inspection of soldered seams in tin cans. Leslie and Wait: power transmission line surveys.
<b>1954.</b> Barnes airborne scanner as a prototype of IR imagers.
<b>1960.</b> IR scanners produce images in 5 minutes.
<b>1961.</b> Detection of overheated components on circuit boards.
<b>1965.</b> AGA (then AGEMA Infrared, now FLIR Systems) introduced the first radiometric IR camera.
<b>1965.</b> Beller: Active TNDT of Polaris rockets. Green: Active TNDT of nuclear fuel elements.
<b>1970s.</b> Balageas, Karpelson**, MacLaughlin, Popov**, Vavilov et al.: 1D, 2D and 3D Thermal NDT models. Use of heat transfer classical solutions.
<b>1973.</b> AGA introduced the first battery-operated portable industrial system, model 750.
<b>1980s.</b> Almond, Berardi, Busse, Carlomagno, Cielo, Favro, Hartikainen, Mandelis, Milne, Rapoport**, Reynolds, Rosencwaig et al.: Thermal wave theory, pulsed TNDT, thermal property measurement. Degiovanni, Maillet et al. introduced «thermal quadrupoles».
<b>1987.</b> A single-piece, thermoelectrically-cooled IR imager with onboard digital image storage introduced by AGEMA, model 470.

<sup>1</sup> vavilov@tpu.ru; phone 7 913 821-9749; fax 7 382 241-7281

<b>1990s.</b> Almond, Balageas, Bison, Bremond, Budadin**, Burleigh, Busse, Cramer, Degiovanni, Grinzato, Krapez, Luong, MacLachlan Spicer, Maldague, Marinetti, Rantala, Vavilov, Walther, Winfree et al.: Practical implementation of TNDT. Development of defect characterization algorithms. IR computerized systems. Study of fatigue phenomena. Various industrial applications. IR thermographic diffusivity and effusivity measurement.
<b>1990s.</b> Uncooled microbolometric IR imagers. Quantum well arrays. A camcorder-style FPA camera from Inframetrics (1995). A low-cost snapshot IR camera from Infrared Solutions (1997).
<b>2000.</b> Thermal/visual/voice and text data logging IR imagers (FLIR Systems ThermaCAM PM 695).
<b>2000s.</b> Avdelidis, Ayvasyan, Balageas, Batsale, Bendada, Busse, Cernuschi, Cramer, Dillenz, Hsie, Maillet, Maldague, Mulaveesala, Nowakowski, Oswald-Tranta, Sakagami, Shepard, Tuli, Więcek, Wu et al.: Commercial Thermal NDT equipment. Novel stimulation techniques. Sophisticated data processing algorithms.
<b>2010s.</b> Maierhofer, Oswald-Tranta, Rajic, Safai, Schlichting, Zalameda et al.: Eddy current IR thermography. Portable equipment for active TNDT.

\* Many researchers who contributed to passive IR thermographic inspection are unfortunately not mentioned, as the emphasis of this paper is active TNDT.

\*\* Earlier Russian publications, not easily available to Western readers [15-17].

Table 2. Pulsed TNDT terminology (in alphabetic order, adapted from [14])

<b>Term</b>	<b>Description</b>
Active IR thermography (active TNDT)*	Infrared thermographic examination of materials and objects that requires additional thermal stimulation.
Ampligram (image of magnitude)	Image that contains pixel-based values of Fourier magnitude at a particular frequency.
Chronological thermogram	Temperature temporal evolution in a particular point.
Defect characterization, (identification, parameters retrieving)	Determining defect parameters by applying inverse algorithms to experimental data.
Temperature difference signal	The difference between the temperature at a current point and a point taken as a reference.
Differentiated contrast	A true temperature is corrected by the theoretical value determined on the basis of the classical solution for adiabatic heating of a semi-infinite body) [18]*.
Direct TNDT mathematical problem	Temperature evolution in space and time is calculated by known sample geometry and material thermal properties.
Dynamic thermal tomography	Tomographic presentation of objects by analyzing temperature temporal evolution in a front-surface test.
Early detection time	A time $\tau^*$ when a temperature signal $\Delta T(\tau)$ starts to exceed a level of noise (typically, $\tau^*$ is much shorter than the optimum observation time $\tau_m$ ).
Infrared thermographic testing (thermographic testing)*	Inspection of materials and products using <i>infrared thermography</i> .
Infrared thermography (IR thermography)*	Imaging an object by sensing the infrared (thermal) radiation emitted by it.
Infrared (IR) thermogram*	A thermal map or image of a target where the grey tones or colors represent the distribution of infrared thermal radiant energy emitted by the surface of the target.
Inverse TNDT problem	Sample/defect thermal properties and geometrical parameters are determined by experimentally measured temperature evolution in space and time.
Maxigram	Image that contains pixel-based maximum values of a chosen meaningful parameter (differential temperature signal) independently of the time of their appearance.
Normalized temperature contrast	Obtained by dividing each image in a sequence by a chosen (normalizing) image. This technique may suppress uneven heating patterns.

Term	Description
Optimum observation time	A time $\tau_m$ when a maximum value of a chosen decision-making parameter, e.g. signal-to-noise ratio, appears.
Phasegram	Image that contains pixel-based values of Fourier phase at a particular frequency.
Polynomial fitting	Fitting noisy temporal evolution functions with polynomial functions (a source sequence of arbitrary length can be replaced with few <i>images of polynomial coefficients</i> ).
Principal component analysis (PCA)	A kind of <i>singular value decomposition</i> .
Pulse phase thermography (PPT)*	Processing technique used in <i>pulsed thermography</i> in which data are analyzed in the frequency domain rather than in the time domain.
Pulsed thermography*	Active infrared thermographic inspection technique, in which a test sample is stimulated with a pulse of energy and recorded infrared image sequences are analyzed to enhance defect 'visibility' and to characterize defect parameters.
Reflection mode (front-surface, one-sided test)	Thermal stimulation and temperature monitoring occur on the same sample surface.
Running temperature contrast	Temperature difference signal divided by the excess temperature at the same point. This parameter is independent of absorbed energy.
Singular value decomposition (SVD)	Calculation of a covariation matrix and its eigenvectors of input data. Eigenvectors are placed in order of their magnitude, thus providing components of an analyzed statistical set. By neglecting low-order components, it is possible to improve results, by reducing the effect of such things as uneven heating.
Spatio-temporal filtering (STF)	The algorithm involves simultaneous spatial and temporal filtering to enhance the sig Input parameters are thermal diffusivity and sample thickness or maximum depth of detection [19].
Stimulated (forced, active, transient) TNDT	Additional thermal stimulation is applied.
Synthetic signal processing	A data processing technique patented by Shepard [20] that involves: 1) polynomial fitting; 2) restoring a source function by polynomial coefficients; 3) analysis of temperature derivatives in time.
Synthetic thermal time-of-flight technique (STTOF)	This data processing technique was proposed by Ringermacher et al. [21]. It involves the determination of inflection points in $\Delta T(\tau)$ curves that allows the conversion of temperature images into depthgrams.
Thermal/Infrared NDT	See <i>infrared nondestructive testing</i> .
Thermal tomography*	A data processing technique used in pulsed thermography in which data is analyzed in comparison with a particular time of interest, such as the time of maximum thermal contrast.
Thermal tomogram	Image that contains pixel-based values of thermal properties (defect indications) within a chosen material layer.
Thermal wave imaging*	An active infrared thermographic inspection technique, in which a test sample is heated with periodic pulses of thermal energy. The term is applied to pulsed heating as well.
Thermographic signal reconstruction (TSR)*	A signal-processing technique for reconstructing and improving time-resolved thermal images, used in pulsed thermography testing and based on polynomial fitting of temperature decay. Note: This is a type of <i>synthetic signal processing</i> [20].
Timegram	Image which contains pixel-based values of a characteristic heat transit times, e.g. <i>optimum observation time</i> .
Transmission mode (rear surface, two-sided) test	Thermal stimulation and temperature monitoring occur on opposite sample surfaces.

Term	Description
Vibrothermography*	Thermographic technique for examining an object where temperature differences are created by mechanical vibrations.
Wavelet thermography	A kind of <i>Pulsed phase thermography</i> implementing the representation of a source temperature function by wavelets.

\* These terms are given in accordance with the ISO # 10878 international standard (1<sup>st</sup> edition 11 January 2013).

\*\* References are given for some recently proposed terms.

## 2. ACTIVE TNDT CONCEPT

The basic concept of TNDT is that a test sample is thermally stimulated and the sample's dynamic temperature is thermographically monitored (Fig. 1). Thermal properties of the sample should be known or determined so they can be used in defect characterization procedures (in some cases, the measurement of thermal properties is a separate task). The choice of a heat source is crucial in providing optimum test conditions especially for specific types of defects. For example, 'kissing' defects can be difficult to detect by applying optical heating. However these, may be detected when stimulated by ultrasonic excitation as they may produce a sufficient amount of thermal energy due to internal friction. Water trapped in an aircraft honeycomb panel can be thermographically detected after the plane lands due to the cooling (or freezing) it experiences at high altitude coupled with its high heat capacity. Cracks in steel are difficult to detect when using optical heating but they may be easily detected using inductive heating.

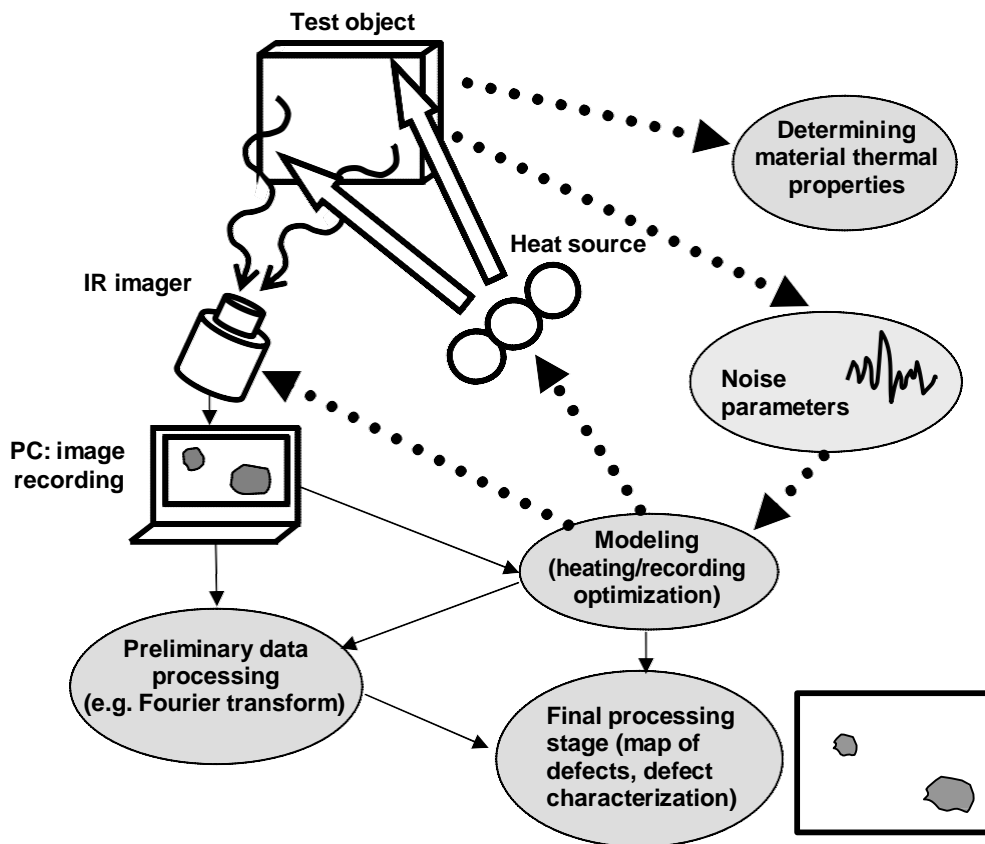


Figure 1. Concept of active TNDT

Any test scheme can be theoretically modeled in order to better understand the mechanism of defect detection and determine the optimal test conditions, such as the power and duration of the heating, IR imager frame frequency and

temperature resolution, etc. Noise characteristics, which are specific for each test object, are important input parameters in modeling. The knowledge of noise amplitude allows evaluation of TNDT limits.

The IR imager provides a sequence of raw IR images, which reflect the dynamic behavior of surface temperatures. Raw IR images can be enhanced ('improved') by applying simple or advanced data processing algorithms. Some algorithms, such as filtration, Fourier and wavelet transform, principle component analysis (PCA), are not linked to the physics of heat conduction. On the other hand, defect characterization algorithms are based on particular thermal models where the analysis of temperature dynamics is crucial.

Ideally, the final test result is a binary map that highlights defects on a uniform background.

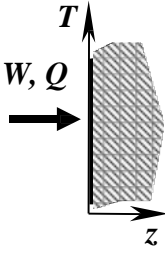
Finally, when using some data inversion procedures, defect depth and thickness can be evaluated. The resultant images may be called "depthgrams" and "thicknessgrams".

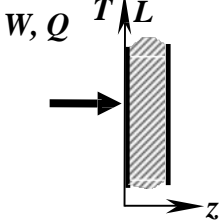
Illustrations of the above are shown in Section 5.

### 3. MODELING IN TNDT

A great variety of solutions to 1D heat conduction can be found in the seminal book of Carslaw and Jaeger [22] and other later monographs. However, many of the solutions are difficult to use because they are too general. The solutions that are widely used in TNDT are often limited to adiabatic models where a semi-infinite body or plate is heated by a heat flux which can be described mathematically as a step, square pulse or Dirac-pulse function. These solutions are shown in Table 3 in a convenient, useful form.

Table 3. Classical TNDT solutions (adiabatic test samples)

Test scheme	Solution
<i>Semi-infinite body</i>	
<p><math>W</math> - absorbed energy, <math>J\ m^{-2}</math>; <math>e = \sqrt{KC\rho}</math> - effusivity (thermal inertia), <math>W\ s^{1/2}\ m^{-2}\ K^{-1}</math>;  <math>K</math> - thermal conductivity, <math>W\ m^{-1}\ K^{-1}</math>; <math>C</math> - specific heat, <math>J\ kg^{-1}\ K^{-1}</math>; <math>\rho</math> - density, <math>kg\ m^{-3}</math>;  <math>a = K/(C\rho)</math> - thermal diffusivity, <math>m^2\ s^{-1}</math>; <math>\alpha</math> - heat exchange coefficient, <math>W\ m^{-2}\ K^{-1}</math></p>	
	<p>Step-function, Front surface: <math>\frac{T}{Q/\lambda} = 2 \left(\frac{a\tau}{\pi}\right)^{1/2}</math></p> <p>Square pulse, Front surface: <math>\frac{T}{Q/K} = 2\left(\frac{a\tau}{\pi}\right)^{1/2} - 2\left[\frac{a(\tau - \tau_h)}{\pi}\right]^{1/2}</math></p> <p>Dirac pulse (flash), Front surface: <math>\frac{T}{W} = \frac{1}{e\sqrt{\pi\tau}}</math>; <math>e = \sqrt{C\rho K}</math></p> <p>Harmonic function: (<math>Q = Q_m \cos(\omega\tau)</math>):  <math>\frac{T(z=0, \tau)}{Q_m} = \frac{1}{K\sqrt{\omega/a}} \cos[\omega\tau - \Theta]</math>, <math>\Theta = 45^\circ</math>.</p> <p>Point-like non-moving source:  <math>\frac{T}{W'} = \frac{1}{4(\pi a \tau)^{3/2}} e^{-4a\tau}</math>, <math>r^2 = x^2 + y^2</math></p> <p>Gaussian non-moving source:  heat energy distribution in space: <math>e^{-(x^2+y^2)/2R^2}</math>;</p>

	$T(r, z=0, \tau) = \frac{W}{2\pi e\sqrt{a\tau}} \int_0^{+\infty} J_0(\sigma r) e^{-\frac{\sigma^2 R^2}{8}} \times$ $\times [\operatorname{erf}(\sigma\sqrt{a\tau}) - \Theta(\tau - \tau_h) \operatorname{erf}(\sigma\sqrt{a} \sqrt{\tau - \tau_h})] d\sigma; \quad r^2 = x^2 + y^2;$ $\Theta(\tau - \tau_h) - \text{step-function (Heviside)}; \quad J_0 - \text{Bessel function.}$
	<p>Step function, Front surface: <math>T = \frac{QL}{K} (Fo + \frac{1}{3} - \frac{2}{\pi^2} \sum_{n=1}^{\infty} \frac{1}{n^2} e^{-n^2\pi^2 Fo})</math>.</p> <p>Rear surface: <math>T = \frac{QL}{K} (Fo - 1 - \frac{2}{\pi^2} \sum_{n=1}^{\infty} \frac{-1^n}{n^2} e^{-n^2\pi^2 Fo})</math>.</p> <p>Square pulse, Front surface: <math>T = \frac{QL}{K} [Fo_h + \frac{2}{\pi^2} \sum_{n=1}^{\infty} \frac{1}{n^2} e^{-n^2\pi^2 Fo} (e^{n^2\pi^2 Fo_h} - 1)]</math>.</p> <p>Rear surface: <math>T = \frac{QL}{K} [Fo_h + \frac{2}{\pi^2} \sum_{n=1}^{\infty} \frac{-1^n}{n^2} e^{-n^2\pi^2 Fo} (e^{n^2\pi^2 Fo_h} - 1)]</math>.</p> <p>Dirac pulse (flash), Front surface: <math>T = \frac{Wa}{KL} (1 + 2 \sum_{n=1}^{\infty} e^{-n^2\pi^2 Fo})</math>.</p> <p>Rear surface: <math>T = \frac{Wa}{KL} [1 + 2 \sum_{n=1}^{\infty} (-1)^n e^{-n^2\pi^2 Fo}]</math>.</p> <p>Harmonic function, Front surface, Non-adiabatic case (<math>Q = Q_m \cos(\omega\tau)</math>):</p> $\frac{T}{Q_m / \alpha} = A_0 \cos(PdFo - \Psi); \quad A_0 = (N_i N_{-i})^{1/2};$ $\Psi = \operatorname{Arctg} \left( i \frac{N_i - N_{-i}}{N_i + N_{-i}} \right); \quad N_i = \frac{ch \sqrt{iPd}}{ch \sqrt{iPd} + (1/Bi) \sqrt{iPd} sh \sqrt{iPd}};$ $N_{-i} = \frac{ch \sqrt{-iPd}}{ch \sqrt{-iPd} + (1/Bi) \sqrt{-iPd} sh \sqrt{-iPd}}; \quad Bi = \frac{\alpha L}{K}; \quad Pd = \frac{\omega L^2}{a}.$ <p>Point-like non-moving source, Front surface::</p> $T = \frac{Wa}{KL 4\pi a L \tau} e^{-\frac{r^2}{4a\tau}} (1 + 2 \sum_{n=1}^{\infty} e^{-n^2\pi^2 Fo}); \quad r^2 = x^2 + y^2.$ <p>Gaussian non-moving source, Front surface:</p> $T(r, z=0, \tau) = \frac{2W}{\pi \rho CL (R^2 + 8a\tau)} e^{-\frac{r^2}{R^2 + 8a\tau}} (1 + 2 \sum_{n=1}^{\infty} e^{-\frac{n^2\pi^2 a\tau}{L^2}}); \quad r_2 = x_2 + y_2.$

Analytical solutions in Table 3 do not include defect parameters. To analyze defects, one must implement either analytical multi-layer, or numerical models.

A short description of available software is given in Table 4. When using these commercial software packages, difficulties may arise in modeling 3D non-linear and pulse heating situations. Specialized programs may be less flexible but may be faster and more applicable to specific problems..

Table 4. General-purpose commercial packages for performing thermophysical calculations\*

Program/ Web site	Feature**
General purpose programs	
Abaqus Unified FEA <a href="http://www.3ds.com/products-services/simulia/products/abacus/">www.3ds.com/products-services/simulia/products/abacus/</a>	Finite element method Vehicle loads, dynamic vibration, multi-body systems, impact/crash, nonlinear static, thermal coupling, and acoustic-structural coupling
Adina (Automatic Dynamic Incremental Nonlinear Analysis) System <a href="http://www.tdoglobal.com/Distribution-Adina-Software">www.tdoglobal.com/Distribution-Adina-Software</a>	A set of programs for static and dynamic displacement and stress analyses of solids, structures and fluid structure systems
Algor/Multiphysics <a href="http://www.algor.com/products/analysis_replays/">www.algor.com/products/analysis_replays/</a>	Transient coupled fluid flow and thermal analysis
Ansys/Multiphysics <a href="http://www.ansys.com">www.ansys.com</a>	General purpose software Finite element method Graphical data processor
CosmosM/HSTAR <a href="http://www2.htw-dresden.de/~fem/Docs/COSMOSM/HSTAR.pdf">www2.htw-dresden.de/~fem/Docs/COSMOSM/HSTAR.pdf</a>	Controlled numerical grid 2D & 3D geometry
Comsol Multiphysics <a href="http://www.comsol.com/comsol-multiphysics">http://www.comsol.com/comsol-multiphysics</a>	General purpose software, based on advanced numerical methods, for modeling and simulating physics-based problems Transient heat transfer Thermal properties dependent on temperature
Marc <a href="http://www.mssoftware.com/product/marc">http://www.mssoftware.com/product/marc</a>	General purpose software, nonlinear finite element analysis Static, dynamic and multi-physics loading Anisotropic materials Heat exchange by convection and radiation
Matlab/PDE <a href="http://www.mathworks.com/products/matlab/">http://www.mathworks.com/products/matlab/</a>	General purpose software Smart power grid Boundary conditions dependent on time Layers separated by a thermally-resistive gap
MSC-Nastran <a href="http://www.macsch.com">www.macsch.com</a>	General purpose software, finite element analysis
Samsef/Thermal <a href="http://www.samsef.com">www.samsef.com</a>	Signatures of IR radiation in typical wavelength bands
Mathematica SmartCAE Heat Transmission <a href="http://www.wolfram.com/products/applications/smartcae/">http://www.wolfram.com/products/applications/smartcae/</a>	General-purpose software Calculation of steady and transient heat conduction
MuSES, RadTherm, WinTherm <a href="http://www.thermoanalytics.com">www.thermoanalytics.com</a>	Thermal and infrared analysis software modules

Specialized modeling programs (Innovation, Ltd.)	
Layer-3 Analytic	Analytical solution for heating a 1D three-layer non-adiabatic plate with a square pulse
Multilayer-3D	Numerical solution for heating a 1D multi-layer plate, arbitrary heating function and phase transformation in an internal layer
ThermoCalc-2D	Numerical solution for heating a 2D three-layer disk-like body with a concentric defect (cylindrical geometry) Heating with a square or harmonic pulse Thermal wave heating Adaptive convection & radiation
ThermoCalc-36L	Numerical solution for heating a 3D 36-layer parallelepiped-like body with up to 9 parallelepiped-like defects (Cartesian geometry) Layer thermal property tensor can be oriented in space under a particular angle Heating with a square or harmonic pulse Arbitrary heating function in time/space All model parameters are arbitrary functions of time Spatial heat mask (artificial or experimental) Producing IR image sequences
ThermoSource	Similar to ThermoCalc-36L, but with internal heat sources

- \* Some data: courtesy of E. Grinzato.
- \*\* Some features apply to particular programs only.

#### 4. BASIC FEATURES OF ACTIVE TNDT

A schematic of classical TNDT, including the thermal response of both sides of the sample, is shown in Fig. 2a. A sample is stimulated on the surface with power  $Q$ ,  $\text{Wm}^{-2}$  (flash stimulation is described with the energy  $W$ ,  $\text{Jm}^{-2}$ ). Temperatures  $T_d, T_{nd}$  are in defect and non-defect areas respectively. The temperature difference,  $\Delta T = T_d - T_{nd}$ , that appears over (or under) a defect, is a natural detection parameter that is linearly proportional to  $Q$  (Fig. 2b). The running temperature contrast  $C = \Delta T / T_{nd}$  is independent of  $Q$  (Fig. 2b).

The basic features of active TNDT are presented in Figs. 2c-l for both the front and rear surfaces.

Temperature difference signals  $\Delta T$  in all cases reach maximums at the corresponding optimum observation times  $\tau_m$  (Fig. 2c, d). Temperature contrasts  $C$ , behave in the same way but on the rear (R)-surface, its maximum typically appearing at very early times when both  $\Delta T$  and  $T$  tend to zero (Fig. 2c, d). Therefore, in a two-sided procedure, an optimum observation time should be chosen as early as possible when the corresponding  $\Delta T$  only starts to exceed noise.

Front (F)-surface signals strongly decay with defect depth  $l$  (Fig. 2e) but remain relatively the same in the case of a two-sided (R) procedure (Fig. 2f).

Respectively,  $\tau_m$  values increase considerably with  $l$  on the F-surface (Fig. 2g) and are weakly dependent of  $l$  on the R-surface (Fig. 2h).

Dependencies of  $\Delta T_m$  and  $\tau_m$  on defect thickness  $d$  and lateral size  $h$  reveal saturation on both F- and R-surfaces,  $C_m$  (Figs. 2i-l). The interesting feature here is that  $\tau_m$  values are more stable against variations of  $d$  and  $h$ . In conjunction with lower noise in the time domain, this makes time parameters preferable in active TNDT.



<p><b>Data fusion</b>  Combining TNDT and other NDT techniques makes sense if: 1) TNDT serves as a screening technique which forestalls using other, presumably, more reliable techniques, 2) inspection hardware is characterized by mutual components, such as a heater, and 3) data fusion is not a simple summation but leads to a new quality of inspection.</p>	<p>Defect detection and characterization may be more efficient due to several physical principles involved.</p>	<p>Data fusion algorithms are not well-explored. Image preparation may be tedious because of different image formats and viewangles.</p>
---	---	--

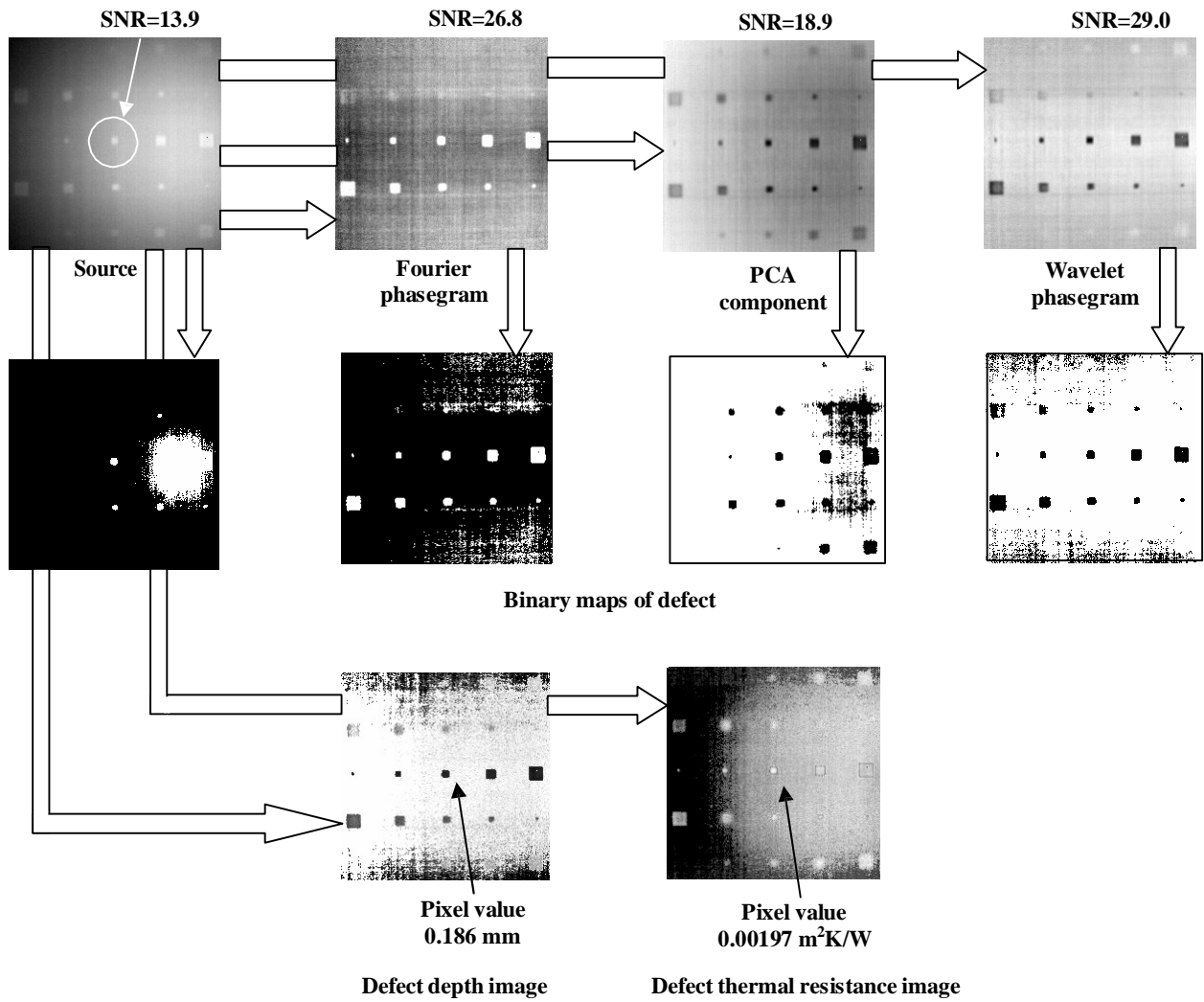


Figure 4. Preliminary and advanced data processing in TNDT (raw images: courtesy of W. Świdorski)

## 6. CONCLUSION

This paper contains reference information on TNDT, including the historical milestones, terminology and data processing algorithms. It is hoped that it will be useful to beginning researchers in TNDT.



Figure 2. Basic active TNDT features:

- a – test scheme,
- b – temperature signal (contrast) vs. stimulation power,
- c,d – time evolution of temperature signal (contrast), e,f – temperature signal (contrast) vs. defect depth,
- g,h- optimum observation time vs. defect depth,
- i,j – temperature signal (contrast) and optimum observation time vs. thickness,
- k,l – temperature signal (contrast) and optimum observation time vs. defect lateral size

## 5. DATA PROCESSING IN TNDT

Data (image) processing algorithms are described in Fig. 3 and Table 5.

Following the TNDT concept in Fig. 1 and the processing scheme in Fig. 3, a raw IR thermogram could first be processed to enhance the signal-to-noise (SNR) ratio, and then converted into a binary map of defects which is preferred by end-users. An example of such a process is shown in Fig. 4 in the application of the inspection of a graphite/epoxy sample. The efficiency of processing algorithms can be evaluated by SNR or visually by viewing defect maps and comparing them with the locations of real defects in a reference sample. Note that defect maps can be produced by thresholding any processed or unprocessed image. In the case of Fig. 4, the best results were obtained by applying the wavelet transform (e.g., for the central defect shown with the circle, the SNR value enhanced from 13.9 in the source image to 29 in the wavelet phasegram). The use of SNR is effective in the inspection of reference samples where the thermographer has to identify non-defect and defect areas and calculate SNR as:

$$S = \frac{\sqrt{\sum_{i=1}^M (T_i - \bar{T}_{nd})^2 / M}}{\sigma_{nd}}$$

where  $T_i$  is the temperature (or any derivative signal) in the  $i$ -th pixel of a defect area,  $\bar{T}_{nd}$  is the mean temperature in a non-defect area, and  $M$  is the number of pixels in a chosen defect area.

It is important to point out that SNR values are related to pixel amplitudes and thus do not take into account the temperature pattern shape and size. The latter parameters are best evaluated by an operator and defects may be detected on a noisy background even if  $SNR \leq 1$ .

Combining the raw data with the corresponding maps of defects allows one to choose regions of interest and characterize defect parameters, for example by producing images of defect depth and thickness, as shown in Fig. 4. Note that, in the depthgram, the central defect depth is 0.186 mm, compared to the true value of 0.2 mm. The corresponding defect thermal resistance value is  $0.00197 \text{ m}^2\text{KW}^{-1}$ ; hence, assuming an air-filled defect with a conductivity of  $0.07 \text{ Wm}^{-1}\text{K}^{-1}$ , and this is equivalent to a defect thickness of 138  $\mu\text{m}$  (the true value is unknown).

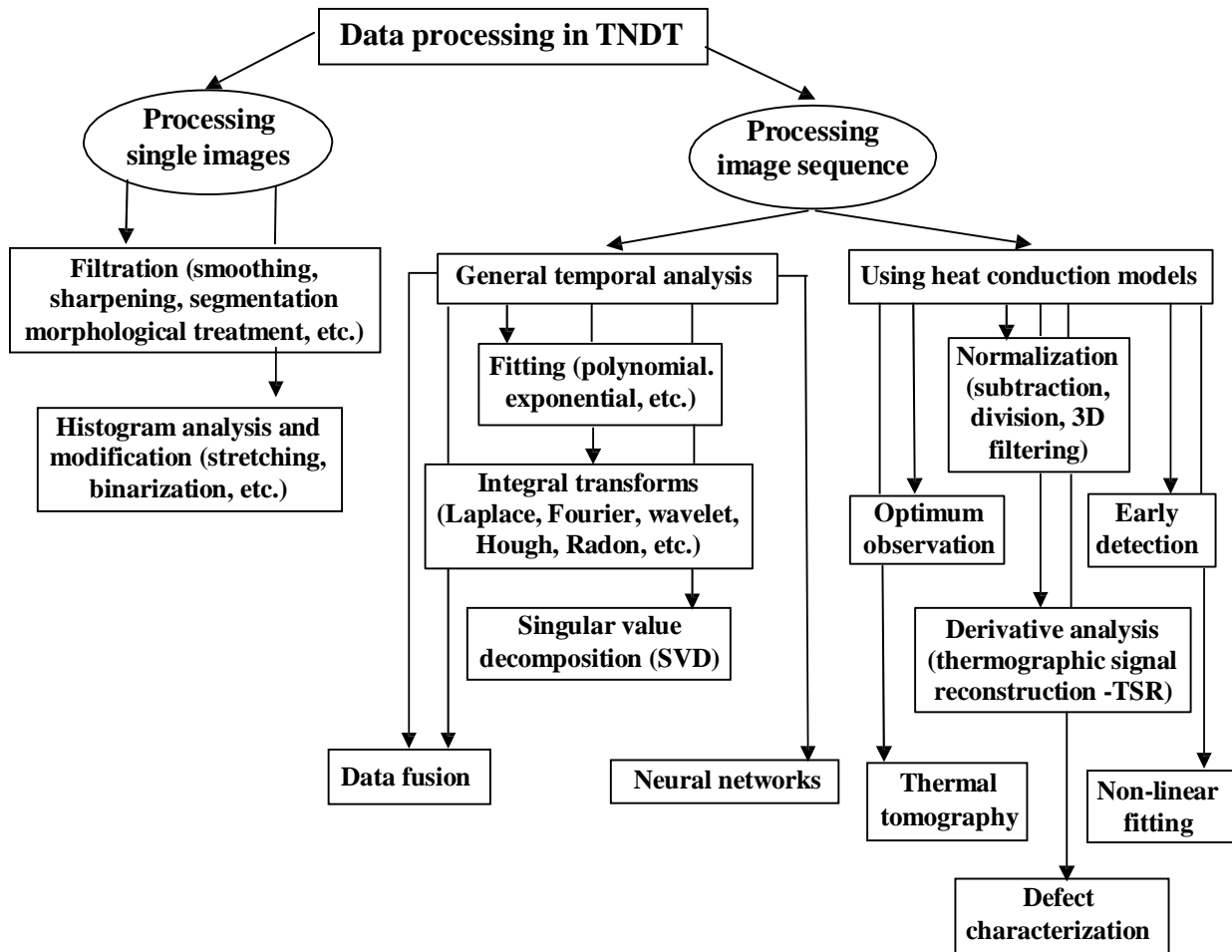


Figure 3. Data processing algorithms in TNDT (adapted from [14])

Table 5. Data (image) processing algorithms in TNDT adapted from [14])

Algorithm and short description	Advantages	Disadvantages
<u>Temperature difference signal</u> The technique allows the evaluation of temperature difference between defect and non-defect areas $\otimes T(x, y, \tau) = T_d - T_{nd}$ .	The technique is naturally related to the physics of TNDT. Smaller and deeper defects produce smaller $\otimes T$ signals.	This technique is susceptible to surface (emissivity/absorptivity) noise. A reference point is necessary.
<u>Running temperature contrast</u> A source temperature image is replaced with the image of the $Con(x, y, \tau) = T_d / T_{nd} - 1$ parameter.	Running contrast is independent of heating power.	This technique may enhance random noise. Lateral heat diffusion is not taken into account. A reference point is necessary.
<u>Differentiated contrast</u> This technique assumes that at earlier times, any sample behaves as a semi-infinite body. The calculated parameter is	No reference point is necessary.	The technique is applicable for shallow defects and for a sample that can be considered as a semi-infinite body.

$C^{dif}(x, y, \tau^{(n)}) = T(x, y, \tau) - \sqrt{\frac{\tau^{(n)}}{\tau}} T(x, y, \tau^{(n)}),$ <p>where <math>\tau^{(n)}</math> is the time taken for normalization [20].</p>		
<u>Averaging</u> The averaging of $N$ images in time reduces random noise by $\sqrt{N}$ times.	Improvement of IR imager temperature resolution.	The technique does not take into account the emissivity/absorptivity noise.
<u>Normalization</u> Dividing each image in a sequence by a chosen (reference) image.	Suppression of uneven heating phenomena.	Random noise may increase. The efficiency is affected by lateral heat diffusion.
<u>Early Detection</u> Defect temperature patterns are analyzed at early observation times.	A lack of significant heat diffusion in lateral directions provides sharp images of hidden defects.	Signal-to-noise ratio is low, so only larger defects may be detected, while smaller ones may not.
<u>Laplace transform</u> Heat diffusion equations and initial/boundary conditions are replaced by a linear matrix equation.	Solving the heat conduction differential equation in the original space is reduced to the solving of algebraic equations in the Laplace domain. Analytical expressions for defect characterization are available.	Heat diffusion is assumed to be 1D. Computation is time-consuming; therefore, defect characterization can be achieved at single pixels.
<u>Fourier transform (pulsed phase thermography)</u> Pulsed TNDT which results in producing images of Fourier phase (phasegrams) and magnitude (ampligrams) by performing 1D Fourier transform in time.	Suppression of uneven heating phenomena. Enhancement of the visibility of deeper defects.	The effectiveness depends on the acquisition interval and image sequence length. Defect characterization is non-trivial.
<u>Wavelet transform</u> Wavelet analysis uses a movable self-adjusting spatial/temporal window and enables the detection of both low- and high-frequency signal characteristics within different time scales [23].	This technique is similar to Fourier transform but allows the localization of a process in time.	The potential of this technique is not fully explored.
<u>Singular value decomposition (SVD), or principal component analysis (PCA)</u> This technique involves the calculation of a covariation matrix of input data, as well as eigenvectors and eigenvalues of this matrix. Eigenvectors are placed by order of their magnitude thus supplying components of an analyzed statistical set.	PCA is used for extracting both spatial and temporal features from IR thermographic sequences of source data. By neglecting low-order components, it is possible to reduce a problem metrics, for example, to exclude the influence of uneven heating or underline particular defects.	Images of principle components lose the physics of heat conduction. Defect characterization is non-trivial.

<p><u>Polynomial fitting</u> Fitting noisy temperature signals with polynomial functions.</p>	<p>A source IR image sequence of arbitrary length can be replaced with images of a few polynomial coefficients.</p>	<p>Images of polynomial coefficients lose the physics of heat conduction. Defect characterization is non-trivial.</p>
<p><u>Thermographic signal reconstruction (TSR)</u> The technique involves polynomial fitting of experimental temperature evolutions and analysis of temperature derivatives [20]</p>	<p>Efficient discrimination between defect and non-defect areas. High image quality.</p>	<p>The technique is applicable to one-sided flash heating procedures for samples which can be considered as a semi-infinite bodies.</p>
<p><u>Correlation</u> A correlation coefficient between time evolutions in each pixel and a chosen reference pixel is calculated [24]</p>	<p>This technique allows good suppression of noise by efficiently discriminating between defect and non-defect areas.</p>	<p>Feasibility of this technique depends on the length of the image sequence . Defect characterization is non-trivial.</p>
<p><u>Dynamic thermal tomography (DTT)</u> Tomographic presentation of objects by analyzing time evolution of surface temperature signals in one-sided TNDT.</p>	<p>Suppression of emissivity/absorptivity noise. Separation of defects by material layer.</p>	<p>The number of separated material layers does not exceed 3-5. A reference point is necessary (some reference-free algorithms have been proposed).</p>
<p><u>Synthetic thermal time-of-flight (STTOF)</u> It is assumed that a defect behaves as a thin plate, while a non-defect area is considered semi-infinite. [21].</p>	<p>Temperature images are converted into depthgrams.</p>	<p>The technique is applicable to a sample which can be considered as a semi-infinite body. A reference point is necessary.</p>
<p><u>Hough transform</u> The technique recognizes patterns (lines) in image by finding geometrical structures [25].</p>	<p>Hough transform discriminates between defect and non-defect areas by assuming the straight-line behavior of temperature in Log-Log coordinates. No reference point is necessary.</p>	<p>The technique is applicable to a sample which can be considered as a semi-infinite body.</p>
<p><u>Radon transform</u> This technique is used to reconstruct images by taking integrals along a straight line which is defined by its slope and line offset [26].</p>	<p>Similarly to Hough transform, this technique discriminates between defect and non-defect areas by assuming the straight-line behavior of temperature in Log-Log coordinates. No reference point is necessary.</p>	<p>The technique is applicable to a sample which can be considered as a semi-infinite body.</p>
<p><u>Neural networks</u> A neural network is a computer program which simulates a set of simple processors with multiple connections. Neural networks are convenient for solving multi-parametric problems.</p>	<p>A universal technique which takes into consideration subtle variations in signal evolution.</p>	<p>Each class of test objects requires special training of the network.</p>

<p><b>Data fusion</b>  Combining TNDT and other NDT techniques makes sense if: 1) TNDT serves as a screening technique which forestalls using other, presumably, more reliable techniques, 2) inspection hardware is characterized by mutual components, such as a heater, and 3) data fusion is not a simple summation but leads to a new quality of inspection.</p>	<p>Defect detection and characterization may be more efficient due to several physical principles involved.</p>	<p>Data fusion algorithms are not well-explored. Image preparation may be tedious because of different image formats and viewangles.</p>
---	---	--

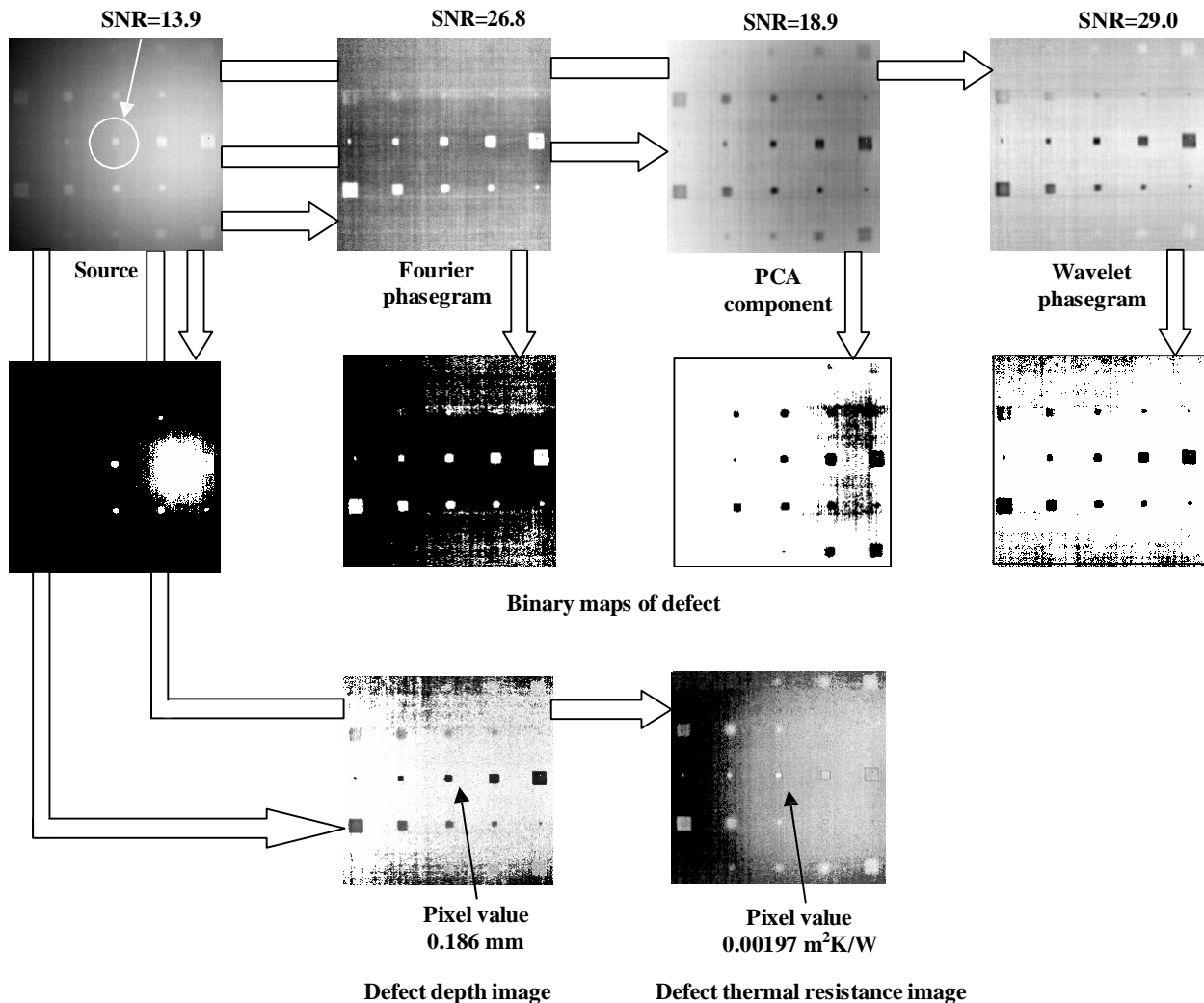


Figure 4. Preliminary and advanced data processing in TNDT (raw images: courtesy of W. Świdorski)

## 6. CONCLUSION

This paper contains reference information on TNDT, including the historical milestones, terminology and data processing algorithms. It is hoped that it will be useful to beginning researchers in TNDT.

This research was supported in part by NIR # 445 (ONG), State order of the Russian Ministry of Higher Education for 2014-2016, and by the grant # 8.1.27.2015 from "The Tomsk State University Academic D.I. Mendeleev Fund Program".

## REFERENCES

- [1] Willburn, D.K., "Survey of infrared inspection and measurement techniques", *Materials Research and Standards* 1, 528-534 (1961).
- [2] McGonnagle, W. and Park, F., "Nondestructive testing", *Intern. Science and Technology* 7, 14-20 (1964).
- [3] Hudson, R.D., [Infrared system engineering], New York: Wiley-Interscience, 1-530 (1969).
- [4] Vavilov, V. and Taylor, R., "Theoretical and practical aspects of the thermal NDT of bonded structures", In: *Res. Techn. in NDT*, ed. by R. Sharpe, London, Academic Press, 5, 239-280 (1982).
- [5] Milne, J.M. and Reynolds, W.N., "The non-destructive evaluation of composites and other materials by thermal pulse video thermography", *Proc. SPIE* 520, 119-122 (1984).
- [6] Burleigh, D., "A bibliography of nondestructive testing (NDT) of composite materials performed with infrared thermography and liquid crystals", *Proc. SPIE* 780, 250-255 (1987).
- [7] Maldague, X., [Nondestructive evaluation of materials by infrared thermography], Springer-Verlag, London, 1-440 (1993).
- [8] Maldague, X., [Theory and practice of infrared technology for nondestructive testing], *Wiley Series in Microwave and Optical Engineering*, New York, John Wiley & Sons, 1-704 (2001).
- [9] Maldague, X. and Moore, P., [Nondestructive Testing Handbook – Infrared and Thermal Testing], *American Society for Nondestructive Testing*, 3, 244-285 (2001).
- [10] Vavilov, V.P., "Pulsed thermal NDT of materials: Back to basics", *Nondestr. Testing & Evaluation* 22(2-3), 177-197 (2007).
- [11] Vavilov, V., [Thermal/Infrared Testing], *NDT Handbook*, Spektr Publishing House, Moscow, 167-222 (2006).
- [12] Vollmer, M. and Möllmann, K.-P., [Infrared thermal imaging: Fundamentals, research and applications], Wiley-VCH, Weinheim, Germany, 1-611 (2010).
- [13] Vavilov, V.P., "Thermal NDT: historical milestones, state-of-the-art and trends", *QIRT. J.* 11(1), 66-83 (2014).
- [14] Vavilov, V.P. and Burleigh, D.D., "Review of pulsed thermal NDT: Physical principles, theory and data processing", *NDT & E International*, 2015 (in press, accepted paper).
- [15] Popov, Yu.A., Karpelson, A.E. and Stokov, V.A., "Thermal NDT of multi-layer structures", *Defectoscopyia (Soviet J. NDT)* 3, 76-81 (1976) (in Russian).
- [16] Kush, D.V., Rapoport, D.A. and Budadin, O.N., "Inverse problem of automated thermal NDT", *Defectoscopyia (Soviet J. NDT)* 5, 64-68 (1988) (in Russian).
- [17] Bekeshko, N.A., Popov, Yu. A. and Upadyshev, A.B., "A plasmatron as a source of localized heating in thermal nondestructive testing of materials and products", *Defectoscopyia (Sov. J. NDT)* 5, 88-91 (1972) (in Russian).
- [18] Pilla, M., Klein, M., Maldague, X. and Salerno A., "New absolute contrast for pulsed thermography", *Proc. QIRT 2002 (Quantitative Infrared Thermography)*, Dubrovnik, Croatia, 24-27 Sept., 53-58 (2002).
- [19] Alsaadawi, Z. and Netzelmann, U., "Spatio-temporal filtering of active thermography data for noise reduction and data compression", *Proc. QIRT 2010 (Quantitative Infrared Thermography)*, Québec, Canada, 27-30 July, 1-8 (2010).
- [20] Shepard, S., "Advances in pulsed thermography", *Proc. SPIE* 4360, 511-515 (2001).
- [21] Ringermacher, H.I., Howard, D.R. and Knight, B., "Thermal imaging NDT at General Electric", *Proc. 18th WCNDT*, 16-20 April 2012, Durban, South Africa, 1-4 (2012).
- [22] Carslow, H.S. and Jaeger, T.S., [Conduction of heat in solids], Oxford Univ. Press, Oxford, U.K., 1-580 (1959).
- [23] Galmiche, F., Vallerand, S. and Maldague, X., "Wavelet transform applied to pulsed phase thermography", *Proc. V-th Workshop on Advances in Infrared Technology and Applications*, ed. by E. Grinzato, P. Bison and A. Mazzoldi, CNR, Venice, Italy, 117-122 (1999).
- [24] [ThermoFit Pro operation manual], Tomsk, Russia, Innovation, Ltd., 1-87 (2002).
- [25] Ibarra-Castanedo, C., Gonzalez, D., Galmiche, F., Maldague, X.P. and Bendada, A., "Discrete signal transforms as a tool for processing and analyzing pulsed thermographic data", *Proc. SPIE* 6205, 620514-1-12 (2006).
- [26] Gonzales, D., Ibarra-Castanedo, C., Madruga, F. and Maldague, X.P., "Analysis of pulsed thermographic sequences based on Radon transform", *Proc. SPIE* 6205, 62051N-1-7 (2006).